FIELD-EMISSION CATHODES FOR FREE-ELECTRON LASERS

J. D. Jarvis, H. L. Andrews, C. A. Brau, B. K. Choi, J. Davidson, B. Ivanov, W.-P. Kang, C. L. Stewart, and Y.-M. Wong, Vanderbilt University, Nashville, TN, U.S.A.

Abstract

High-quantum-efficiency (QE) photocathodes used for free-electron lasers tend to be fragile and demand complex drive lasers. Field-emitter arrays eliminate both these problems, but introduce other problems along with interesting new physics. Diamond field-emitter arrays (DFEAs) are rugged and forgiving of poor vacuum. They are easily conditioned to give uniform emission, current density on the order of 100 A/cm^2 before phase compression, and emittance smaller than 10 μm-radians for a 1 cm cathode. In gated versions the emission can be phased to the rf drive and the emittance can be reduced by the focusing effect of the gate. Experimental evidence from diamond pyramids and carbon nanotubes suggests that field emission is enhanced by resonant tunneling through molecules adsorbed on the surface. The emission from individual molecules appears to reach the fundamental limits imposed by the Heisenberg uncertainty principle and by the Pauli exclusion principle.

BACKGROUND

Photocathodes have been extremely important to the development of free-electron lasers (FELs). The metal photocathode variety has low QE but is typically robust and reliable. In contrast, semiconductor photocathodes have very high QE but surface condition is extremely important and they are easily poisoned. Alkali-coated-metal photocathodes have a reasonably high QE but are also susceptible to contamination. Accordingly, they must be prepared *in situ* and require load-lock systems that interface with the injector. A notable exception is the dispenser type cathode in which the alkali element is bound up in a relatively inert compound. Photocathodes also require complex drive-laser systems and necessitate the inclusion of a laser window in the accelerator design.

Field emitter arrays offer an interesting alternative to photocathodes. They eliminate the need for drive lasers and a laser window, can provide high current densities before phase compression, and can be time gated with a variety of techniques, including with self-aligned gate electrodes. The transverse emittance is small enough for many FEL applications and can be further reduced by the use of multiple gates for beam collimation. There are several important beam properties to consider when integrating field emitter arrays into electron injector systems for FELs: emission uniformity (temporal and spatial), transverse emittance, lifetime, and emitted energy spectrum. In these proceedings we detail recent progress in the development of DFEAs as beam sources for FELs. We discuss pulsed conditioning and high current operation, normalized-transverse-emittance measurements, and energy-spectrum measurements.

PULSED CONDITIONING AND OPERATION

Conditioning experiments were performed in a high-vacuum test stand with a base pressure of about 10^{-8} Torr. The system is capable of applied voltages up to 5 kV and electric fields up to 40 V/μm by using 170-330 μm quartz capillaries to space the anode and cathode. A high voltage pulser is connected to the anode and can operate with arbitrary pulse duration from microsecond to DC. A schematic representation of the experimental arrangement is shown in Fig. 1.
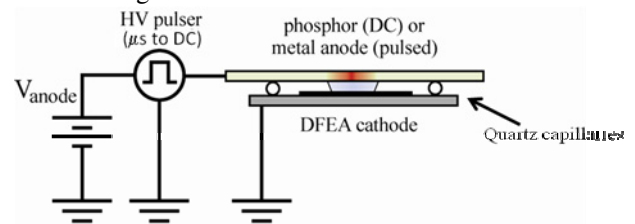

Figure 1: schematic representation of the close diode testing arrangement for pulsed conditioning

Several DFEAs were used in these experiments: a 224×224 array with a 14- μm pitch, a 448×224 array with a 20-μm pitch, and a 20×250 array with a 4-μm pitch. When operated at several microamps per tip, the nanotips on the diamond emitters begin to dull due to thermal-assisted field evaporation [1]. The sharpest tips have the highest joule heating as well as the greatest field stresses, therefore they have higher evaporation rates. This leads to self-limiting conditioning of the array and a high degree of spatial uniformity. For dense arrays DC conditioning is not possible due to anode destruction.
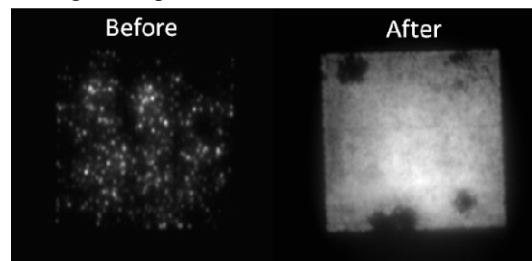

Figure 2: 224x224 array before and after pulsed conditioning

To prevent anode damage the emission can be pulsed at microsecond time scales. Figure 2 shows a low current (~50 μA total) phosphor image of the beam from a 224×224 array (3.14× 3.14 mm) before and after pulsed conditioning at several microamps per tip.
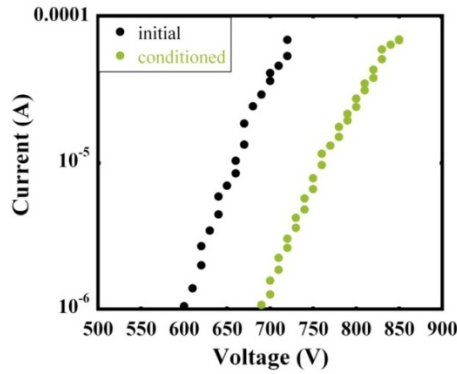
Figure 3: low current IV curves for a 224x224 array before and after conditioning

Low current IV curves are shown in Fig. 3 for measurements before and after conditioning. Clearly it is possible to achieve dramatic uniformity improvements in exchange for marginal increases in the turn-on field. Peak current pulses of 0.6 A were achieved for this array and for a 448×224. A current vs. time trace for the latter is shown in Fig. 4. In pushing to higher total current density we have performed pulsed testing on a 20×250, 4-μm pitch array at a peak current of approximately 25 mA. This corresponds to a current density of about 30 A/cm^2. We would note that this operation was limited by the voltage range of our pulser, and that per-tip currents three times greater have been observed in testing of other arrays. For this same level, the current density would approach 100 A/cm^2.
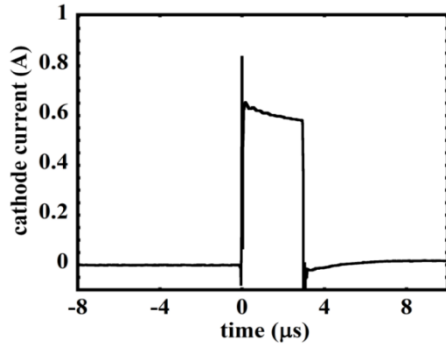

Figure 4: Current vs. time for a 224x448 array operating at a peak current of ~0.6 A

EMITTANCE MEASUREMENTS

To measure the transverse emittance from DFEAs we employ a simple pepperpot technique. The experimental arrangement is shown in Fig. 5. A 1-mm pitch pepperpot with ~50-μm hole size was fabricated by femtosecond laser machining of steel shim stock. The cathode and pepperpot were separated by a distance of 230 μm. The anode cathode voltage for this measurement was 1.3 kV. The beamlets passed by the pepperpot drift for 3.55 mm before impacting the phosphor screen.
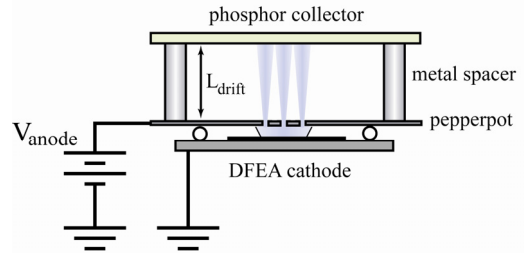

Figure 5: schematic of the experimental arrangement during pepperpot emittance measurements

Figure 5 shows a phosphor image of a beamlet and a horizontal-line scan as well as one of the apertures for size comparison. A Gaussian fit of the beam profile gives an rms angular divergence of 67 mrad, and after correction for the defocusing of the aperture fields, 46 mrad. For a 1x1 mm uniform cathode, the normalized transverse rms emittance is then $\varepsilon_N \sim 0.94$ μm-rad.
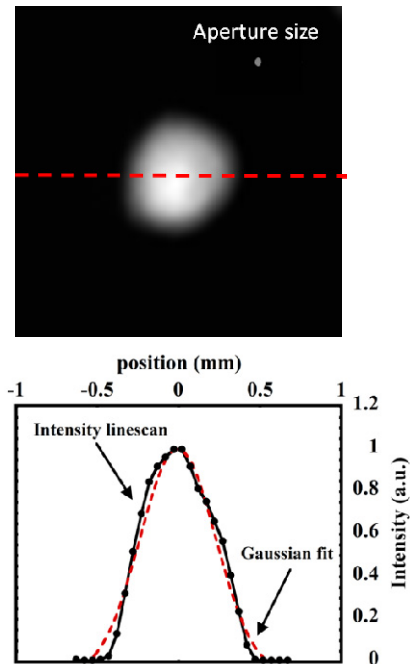

Figure 6: Line scan and gaussian fit of a beamlet from a pepperpot aperture

ENERGY SPECTRUM MEASUREMENTS

All experiments were performed in a UHV test stand with a base pressure of less than 10^{-10} Torr. The system is capable of applied voltages up to 5 kV and electric fields up to 40 V/μm. The cathode holder sits on a gimbaled kinematic mount that allows adjustment of the anode cathode spacing and planarity during operation. The DFEA used in these experiments is a 20×20 array with a pitch of 100 μm.
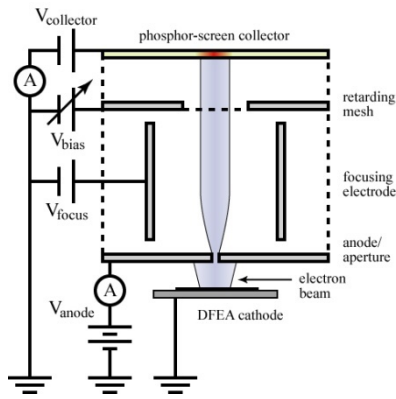
Figure 7: A schematic representation of the energy analyzer/ DFEA system. The 50-μm aperture admits current from a single emitter, which is then collimated and subsequently analyzed with a retarding mesh.

Typical operating parameters were ~ 3 kV anode-cathode voltage, ~ 0.3 mm anode-cathode gap, and ~ 1-100 nA/tip emission current. For an anode-cathode gap less than 0.5 mm, the beamlets from individual emitters are well separated from one another.

When the entire beam is allowed to pass the retarding mesh, the measured collector current exhibits stepwise fluctuations between discrete emission levels as seen in Fig. 8. These changes in current are coincident with spatial intensity fluctuations in the phosphor-screen image. A variety of field emitters including carbon nanotubes (CNTs) and Spindt-type molybdenum cathodes are known to exhibit this same type of emission behavior, and field-emission microscopy has shown that such fluctuations arise from the adsorption, desorption, and diffusion of atoms and molecules on the emitter surface [2-7]. While little is known about the specific emission processes of these diamond tips, in the present experiments the explanation of molecular adsorbtion and diffusion seems to best fit our data, and we analyze them in this context.
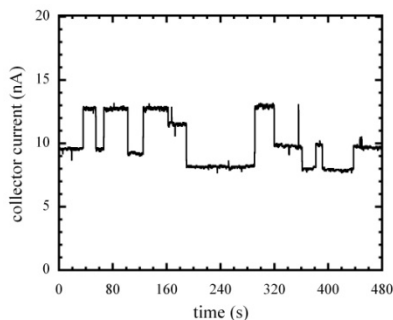

Figure 8: The emission current from an individual CVD diamond field emitter fluctuates between discrete, stable levels. Periods of stability can range from fractions of a second to many minutes depending on the ambient pressure.

All electron-energy spectra presented in this report were taken during periods of stable emission. Figure 9 provides examples of energy spectra that were taken

under identical experimental conditions. Each distinct spectrum corresponds to a period of stability in the total current, similar to those seen in Fig. 8. Transitions between various stable spectra are concurrent with the aforementioned current fluctuations

We have observed spectral features at energies several volts below, and in some cases at fractions of a volt
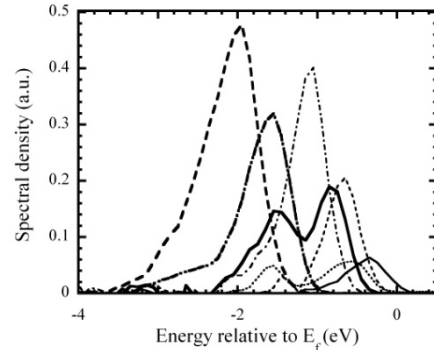

Figure 9: For identical experimental conditions, the emitted energy spectrum fluctuates between a variety of stable configurations. These fluctuations are coincident with those of the emitted current. On occasion, dramatic results were recorded during individual adsorbate events.
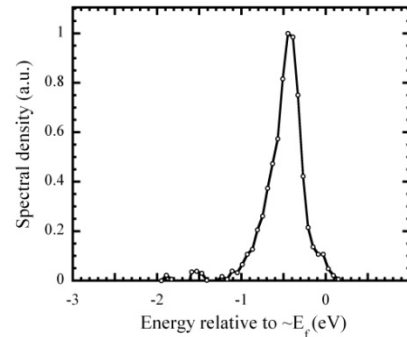

Figure 10: This spectrum is believed to have originated from the clean surface of the CVD-diamond emitter. It is located near the estimated Fermi energy and has a spectral width of ~ 0.3 eV.

above, the Fermi energy. This modification of the emitted electron-energy spectrum is interpreted as the result of resonant tunneling through adsorbed species. For given experimental conditions, we expect that emission from a clean surface should occur at a low intensity near the Fermi energy. Approximately 5-10 percent of the recorded spectra resemble the suspected clean distribution pictured in Fig. 5. The FWHM of this distribution is ~ 0.3 eV, comparable to that of metallic field emitters and similar to what has been measured for various diamond field emitters [8–11]. Figure 10 shows the measured emission spectrum before and after the arrival of a single adsorbate. The emitted current increased by more than an order of magnitude while the spectral width and shape remained unchanged.
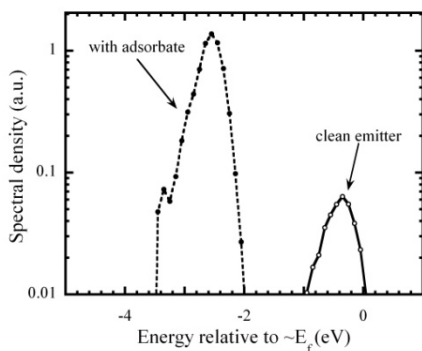
Figure 11: In some cases, single adsorbate events increased the emission current by more than an order of magnitude without affecting the spectral width or shape.
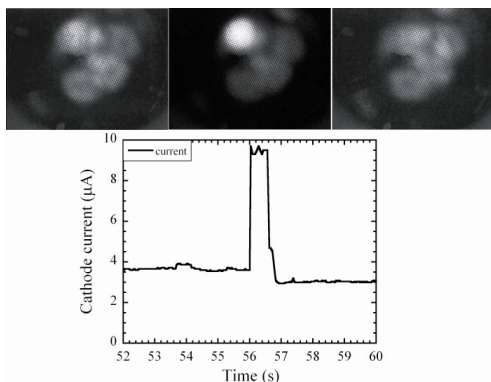

Figure 12: FEM micrograph and I vs. time trace of a nearly quantum degenerate beam from a single adsorbate

NANOTUBES AND DEGENERACY

Because the emission enhancement by an adsorbate is extremely spatially localized, and the energy spread is narrow, field-emitted beams of several microamps may approach the quantum-degenerate limit of electron-beam brightness. At this limit, the beam density in 6-D phase space reaches a maximum and the beam interacts strongly through degeneracy pressure. Such beams may have been observed for short times (~ 1 sec) from residual gases on CNTs. Figure 12 shows an FEM micrograph and current vs. time data for a 6 µA beam from a single adsorbate. By calculating the transverse momentum spread for this beamlet and assuming an energy spread of ~0.3 eV, we estimate that this beam is nearly quantum degenerate. More tightly bound adsorbates such as various metal atoms should stabilize the effect and provide a reliable quantum-degenerate electron beam source. Such a source would represent the ultimate limit of achievable brightness.

CONCLUSIONS

DFEAs continue to demonstrate promise as potential beam sources for free-electron lasers. They are rugged, chemically inert, and have a high thermal conductivity. We have successfully demonstrated pulsed uniformity conditioning at microsecond time scales and have achieved current densities of ~30 A/cm^2 for microsecond pulses. The normalized transverse rms emittance of dense arrays has been measured by a pepperpot technique and was found to be ~1 mm-mrad for a 1x1 mm uniform cathode. Energy spectrum measurements of the emitted beamlets from a single tip have been carried out. We find strong evidence that resonant tunneling through adsorbed atoms and molecules has an important effect on the emission properties of DFEAs. Finally, beams of extraordinary brightness have been observed from individual adsorbates on a MWCNT. We calculate that these beams approach the quantum limit of beam brightness.

REFERENCES

[1] J. D. Jarvis, H. L. Andrews, C. A. Brau, B.-K. Choi, J. L. Davidson, W.-P. Kang, and Y. M. Wong, J. Vac. Sci. Technol. B, To appear in \J. Vac. \Sci. Technol. \B, Sep/Oct 2009.

[2] K. Hata, A. Takakura, and Y. Saito, Surf. Sci. 490 (2001), 296.

[3] A. Wadhawan, R. E. S. Il, and J. M. Perez, Appl. Phys. Lett. 78 (2001), 180.

[4] D.-H. Kim, H.-R. Lee, M.-W. Lee, Y.-H. Song, J.-G. Jee, and S.-Y. Lee,Chem. Phys. Lett. 355 (2002), 53.

[5] R. T. Olson, G. R. Condon, J. A. Panitz, and Pl R. Schwoebel, J. Appl. Phys. 87 (2000), 4.

[6] R. Collazo, R. Schlesser, and Z. Sitar, Diamond and Related Materials 11 (2002), 769.

[7] C. J. Todd and T. N. Rhodin, Surf. Sci. 42 (1974), 109.

[8] A. Ueda, Y. Nishibayashi, and T. Imai, Diamond and Related Materials 18 (2009), 854.

[9] M.-L. Yu, H.-S. Kim, B. W. Hussey, T. H. P. Chang, and W. A. Mackie, J. Vac. Sci. Technol. B 14 (1996), 6.

[10] O. Groening, O. M. Kuttel, P. Groening, and L. Schlapbach, Appl. Phys. Lett. 71 (1997), 16.

[11] C. Bandis and B. B. Pate, Appl. Phys. Lett. 71 (1996), 16.